Soft surfaces and enhanced nonlinearity enabled via epsilon-near-zero (ENZ) media doped with zero-area perfect electric conductor (PEC) inclusions

EHSAN NAHVI[1], IÑIGO LIBERAL[1,2], AND NADER ENGHETA[1,*]

[1] Department of Electrical and Systems Engineering, University of Pennsylvania, Philadelphia, PA 19104, USA.
[2] Department of Electrical, Electronic and Communications Engineering, Public University of Navarra, Pamplona, Spain.
[*] Corresponding author: engheta@ee.upenn.edu

Compiled July 8, 2020

Introducing a dielectric inclusion inside an epsilon-near-zero (ENZ) host has been shown to dramatically affect the effective permeability of the host for a TM-polarized incident wave, a concept coined as photonic doping [Science 355, 1058 (2017)]. In this letter, we theoretically study the prospect of doping the ENZ host with infinitesimally thin perfect electric conductor (PEC) inclusions, which we call "zero-area" PEC dopants. First, we theoretically demonstrate that zero-area PEC dopants enable the design of soft surfaces with an arbitrary cross-sectional geometry. Second, we illustrate the possibility of engineering the PEC dopants with the goal of transforming the electric field distribution inside the ENZ while maintaining a spatially invariant magnetic field. We exploit this powerful property to dramatically enhance the effective nonlinearity of the ENZ host.

http://dx.doi.org/10.1364/ao.XX.XXXXXX

Over the past two decades, epsilon-near-zero (ENZ) media have sparked substantial interest among the metamaterials community, due to their peculiar light-matter interactions[1]. Among the unique properties of such materials is the uniformity of the magnetic field for the TM polarization inside such media when a 2D geometry (i.e. infinitely extended along the out-of-plane direction) is considered. As a result of this powerful feature, it has been theoretically and experimentally shown that "doping" an ENZ host with one or several dielectric dopants enables one to obtain an effectively magnetic ENZ that is characterized by a highly tailorable effective permeability ($\epsilon_{eff} \simeq 0$, $\mu_{eff} \neq 1$). Interestingly, this effective material representation is valid in both the near-field and far-field interactions, and for arbitrarily shaped bodies [2, 3]. The concept of photonic doping has been experimentally demonstrated in rectangular metallic waveguides [3], substrate-integrated waveguides [4], and all-dielectric photonic crystals [5]. In addition, the initial photonic doping idea has been extended and applied to nonlinear optics [6, 7], PT symmetry [8], generalized impedance matching [9], transformation optics [10], and perfect coherent absorption [11].

Typically, the shape and area of a dielectric dopant is designed with the aim of modifying the magnetic flux within the ENZ host, and in doing so controlling the effective permeability. Notably, interesting effects might be observed for dopants with different material and/or geometrical properties. For example, doping the ENZ host with a PEC inclusion, the effective permeability has been shown to depend solely on the ratio between the PEC and ENZ cross-sectional areas[3]. As a corollary, embedding infinitesimally thin PEC dopants inside the ENZ, i.e., "zero-area PEC dopants", would have absolutely no effect on the TM-polarized scattered field from the ENZ body. At the same time, despite being essentially invisible from an outside observer, the presence of zero-area PEC inclusions imposes an extra boundary condition that alters the electric field distribution inside the ENZ. As we numerically illustrate in this Letter, the geometry of the PEC inclusion may be engineered such that the electric field inside the ENZ becomes considerably enhanced. On the other hand, several recent studies have reported huge optical nonlinearity around the ENZ frequency[12–19]. Introducing such engineered PEC dopants inside a nonlinear ENZ host should lead to further enhanced nonlinearity.

Strikingly, while zero-area dopants do not change the external response of the ENZ body to TM waves, they can have an important impact on the response to TE waves. In this manner, they provide the possibility of independently tuning the anisotropic response of a body with a complex geometry. As an example of such anisotropic devices, we investigate electromagnetic soft surfaces, a concept borrowed from acoustics, which was introduced over three decades ago by Kildal[20, 21]. Such surfaces exhibit PEC and perfect magnetic conductor (PMC) behavior for the TE and TM polarizations, respectively[22] and have been utilized for various applications, such as reducing mutual coupling[23] and back radiation[24] of patch antennas. Soft surfaces have been realized by various corrugated metallic surfaces[25] and strip-loaded grounded dielectric slabs[22, 26]. We theoretically demonstrate that judiciously doping ENZ media with zero-area PEC inclusions enables the implementation of 2D structures with soft surfaces with arbitrary cross-sectional geometry while recovering subwavelength details of the fields excited on its boundary.

According to the theory of photonic doping, for the TM po-

larization, introducing a dielectric inclusion inside an arbitrarily shaped 2D ENZ medium allows one to largely tailor the effective permeability, μ_{eff}, while maintaining the effective permittivity near zero, $\epsilon_{eff} \simeq 0$. In particular, assuming the ENZ is doped with a circular dielectric rod, the effective permeability approaches infinity for specific rod radii[3]. In contrast, inserting a zero-area PEC inclusion inside the ENZ medium does not disturb the uniform magnetic field inside the ENZ, and the magnetic flux through the doped ENZ body; thus, leaving μ_{eff} unaffected (see Supplement 1). Hence, by doping an ENZ medium with both a dielectric rod and a zero-area PEC inclusion, in accordance with the schematic depicted in Fig. 1a, the TM-polarized scattered fields may be identical to that from a PMC with identical geometry. For example, in Figs. 1b,1c, for an incident TM-polarized plane wave propagating along the $-\hat{x}$ direction, we numerically confirm that the scattered fields from the doped ENZ are identical to a PMC with identical geometry[27].

However, the photonic doping concept for ENZ media is limited to the TM polarization. In other words, a doped ENZ cannot be accurately described by an effective permittivity and permeability for the TE polarization. We propose exploiting this limitation for obtaining a structure with scattering behavior immensely different for the TE and TM polarizations, namely a soft surface. Even though the zero-area PEC inclusion is essentially invisible for the TM polarization, its presence significantly alters the TE-polarized scattered fields. An interesting situation occurs when a zero-area PEC inclusion conforms with the contour of the ENZ by a small distance $d_{gap} << \lambda_0$, except for a tiny opening with length $d_{opening} << \lambda_0$ that ensures that the PEC body has a zero area. For the TE polarization, the structure is virtually identical to a PEC with a very thin ENZ coating, as confirmed in Figs. 1d,1e. Therefore, in the limiting case of $d_{opening} << \lambda_0$ and $d_{gap} << \lambda_0$, the TE-polarized scattered fields from the doped ENZ become similar to that of a PEC with identical geometry. Hence, such doped ENZ media which are equivalent to a PEC and PMC for the TE and TM polarizations, may be considered as an alternative approach for designing soft surfaces.

In order to obtain further insight into the operation of such structures as soft surfaces, we consider the simple geometry of a slab, as illustrated in Fig. 2a. Assuming the dielectric rod parameters are chosen to satisfy $J_0(k_d r_d) = 0$, the doped ENZ slab is equivalent to a PMC for the TM polarization, resulting in a reflection coefficient $\Gamma_{TM} = +1$ for normal incidence. In contrast, for a TE-polarized normally incident plane wave, assuming the PEC sheet is parallel to the ENZ boundary with electrically small periodic openings (i.e. $w_{PEC} \lesssim w$), the slab is approximately equivalent to a PEC surface with an ENZ coating of thickness d_{gap}. Therefore, upon applying the continuity boundary conditions for the tangential fields and straightforward algebraic manipulations, one finds the reflection coefficient for normal incidence given by (assuming $\exp(-i\omega t)$ convention):

$$\Gamma_{TE} = \frac{i2\pi(d_{gap}/\lambda_0)+1}{i2\pi(d_{gap}/\lambda_0)-1} \quad \textbf{(1)}$$

Decomposing the reflected wave in terms of circularly polarized components, we find the reflection coefficient for the RHCP and LHCP components given by $\Gamma_{RHCP} = (\Gamma_{TM} - \Gamma_{TE})/2$ and $\Gamma_{LHCP} = (\Gamma_{TM} + \Gamma_{TE})/2$, respectively.

As plotted in Fig. 2b, the results obtained from our full-wave simulations closely agree with our approximate analytical expressions which were founded on the premise of a sufficiently small opening in the zero-area PEC inclusion. Moreover, our

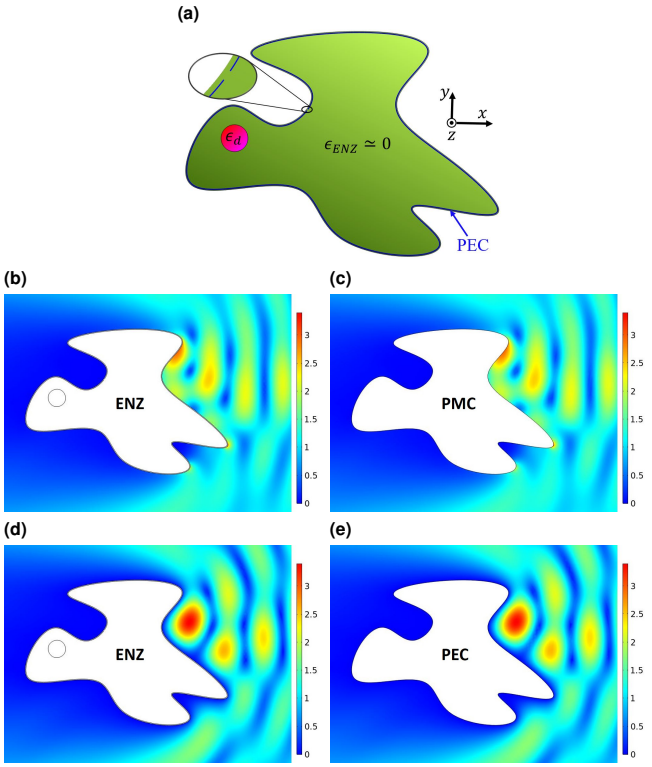

Fig. 1. A soft surface with arbitrary geometry designed using a doped ENZ medium. (a) Geometry of a 2D ENZ with cross-sectional area $A_{ENZ} = 3\lambda_0^2$, doped with a dielectric rod with permittivitiy $\epsilon_d = 9.84$ and radius of $r_d = 0.122\lambda_0$, and a zero-area PEC inclusion with an opening of length $d_{opening} = 0.01\lambda_0$, following the ENZ boundary by a distance of $d_{gap} = 0.01\lambda_0$. An incident plane wave is traveling in the $-\hat{x}$ direction. (b)-(e) Normalized electric field magnitude distribution outside (b) the doped ENZ for the TM polarization. (c) an ideal PMC with identical geometry for the TM polarization. (d) the doped ENZ for the TE polarization. (e) an ideal PEC with identical geometry for the TE polarization.

results corroborate that the handedness of an incident circularly polarized wave is maintained, a hallmark of soft surfaces, as long as the PEC inclusion is sufficiently close to the ENZ boundary.

In addition to designing soft surfaces, judiciously doping ENZ media with zero-area PEC inclusions enables shaping the electric field distribution, and thus significantly enhancing the nonlinear response of ENZ media, which have already been shown to manifest an unprecedentedly large optical nonlinearity[12]. To illustrate this point, we consider an ENZ slab deployed in a single-ENZ-channel impedance matching configuration[9]. The parameters of the arrangement illustrated in Fig. 3a, such as the ENZ and air buffer thicknesses, have been chosen such that the reflection for a normally incident TM-polarized wave is suppressed, without the need for a dielectric inclusion in the ENZ medium. For such a structure, we investigate the effect of a zero-area spiral PEC inclusion on the electromagnetic field distribution inside the ENZ slab.

In accordance with our earlier discussion, for a TM-polarized incident wave, the presence of a PEC spiral does not affect the electromagnetic fields outside the ENZ, as well as the uniform magnetic field inside the ENZ medium (see Figs. 3b,3c). How-

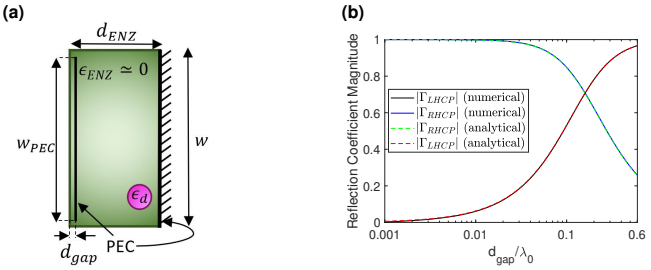

Fig. 2. (a) An RHCP plane wave normally incident from air on a PEC-backed doped ENZ slab behaving as a soft surface. An ENZ slab with thickness $d_{ENZ} = \lambda_0$ is doped with periodicity $w = 2\lambda_0$ by a dielectric rod with permittivity $\epsilon_d = 9.84$ and radius $r_d = 0.122\lambda_0$, in addition to a zero-area PEC sheet inclusion with length $w_{PEC} = 1.96\lambda_0$, separated from the ENZ boundary by a small distance denoted by d_{gap}. (b) Analytically and numerically obtained reflection coefficient amplitude for circularly polarized components as a function of d_{gap}.

ever, the presence of the PEC inclusion imposes an additional boundary condition which may considerably impact the electric field distribution inside the ENZ slab. In the context of the configuration presented in Fig. 3, in the absence of the PEC inclusion, the electric field maintains the same orientation in the ENZ slab and the surrounding media (see Fig. 3d). The presence of the PEC inclusion, however, imposes an extra boundary condition, requiring a vanishing electric field tangential to the spiral, hence modifying the orientation of the electric field inside the ENZ. In fact, with a judicious choice of the geometry of the zero-area PEC inclusion, such as the spiral depicted in Fig. 3a, it is possible to dramatically enhance the electric field in portions of the ENZ medium, as illustrated in Fig. 3e. Although we have not done so in our proof-of-concept numerical demonstration, by optimizing the geometry of the zero-area PEC inclusion, we envision the possibility of enhancing the electric fields even further inside the ENZ.

Intuitively, the enhanced electric field inside a nonlinear ENZ medium, created by the presence of zero-area PEC inclusions, should lead to an enhanced nonlinear response. To verify this intuition, we assign Kerr nonlinearity to the ENZ medium in the configuration depicted in Fig. 3a. Simulating the structure for a range of incident intensities, we confirmed that the presence of the zero-area PEC inclusion indeed leads to boosted nonlinearity, as evident from the nonlinear permittivity averaged over the ENZ, and the reflection coefficient magnitude, plotted in Fig. 4a and Fig. 4b, respectively. As a matter of fact, the nonlinearity has been enhanced to the extent that the highly nonlinear characteristic of hysteresis has emerged. Surprisingly, despite the modest change in permittivity throughout the ENZ, the reflection becomes remarkably large. In fact, as we decrease the incident intensity, we find that for $I_0 \simeq 2.5 \times 10^9\ (W/m^2)$, the incident wave undergoes total reflection. According to our numerical studies, for the incident intensity corresponding to total reflection, despite a modest change in the permittivity over the entire ENZ host, the magnetic field is significantly enhanced inside the spiral. Even though the magnetic field should be uniform inside an ENZ medium, the modest variation in the permittivity allows for a nonuniform magnetic field distribution inside the ENZ for sufficiently large incident intensities (see Supplement 1). It is noteworthy that our approach for boosting the nonlinearity of ENZ media is governed by a completely different mechanism compared to an earlier proposal which exploited the doping of

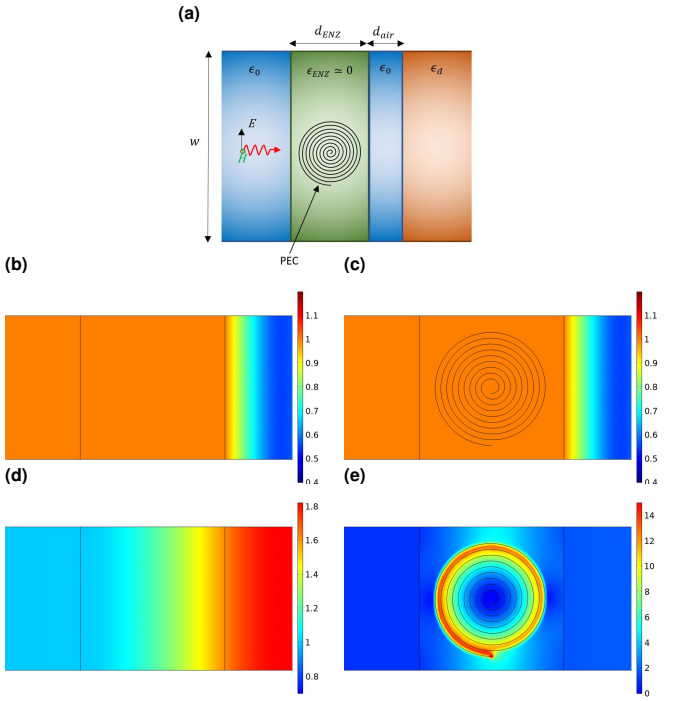

Fig. 3. The effect of a zero-area PEC dopant on the electromagnetic field distribution inside a linear ENZ medium. (a) A TM-polarized plane wave normally incident on an ENZ slab, doped by a zero-area PEC spiral, deployed in a single-ENZ-channel impedance matching configuration[9]. The ENZ slab ($\epsilon_{ENZ} = 10^{-6}$) with thickness $d_{ENZ} = 0.202\lambda_0$ and periodicity $w = 0.2\lambda_0$ is separated from a dielectric substrate with permittivity $\epsilon_d = 11$ by an air gap of thickness $d_{air} = 0.330\lambda_0$. The Archimedean spiral has a final radius of $r_f = 0.4d_{ENZ}$, initial radius of $r_i = 0.1r_f$ and $n_s = 9$ turns (geometry not shown to scale for improved visual representation). (b)-(c) The normalized magnetic field magnitude, $|H_z|/H_0$, in the absence and presence of the PEC dopant is illustrated in (b) and (c), respectively. (d)-(e) The normalized electric field magnitude, $|\vec{E}|/E_0$, in the absence and presence of the PEC dopant is illustrated in (d) and (e), respectively. Note two different scale bars in panels (d) and (e).

a linear ENZ host with resonant nonlinear dielectric inclusions to obtain enhanced magnetic nonlinearity[6, 7].

It is worth noting that ENZ media may exhibit a finite amount of loss. Therefore, we numerically investigated the effect of ENZ loss on the enhanced nonlinearity. As shown in Fig. 5, we found that the enhanced nonlinearity remains notable, even in the presence of realistic levels of ENZ loss. For instance, for $\epsilon''_{ENZ} = 0.03$, which corresponds to the loss of SiC around its plasma frequency in the mid-infrared regime[29], the reflection coefficient from the doped ENZ slab exhibits a considerably stronger dependence on the incident intensity in the presence of the zero-area PEC spiral, indicating substantially enhanced nonlinearity arising from the enhanced electric fields provided by the presence of the PEC inclusion, hence confirming the practicality of our proposal for the ever-increasing endeavors for obtaining enhanced nonlinearity in ENZ media[12].

In conclusion, we have theoretically investigated the prospect of introducing a zero-area PEC inclusion inside an ENZ medium

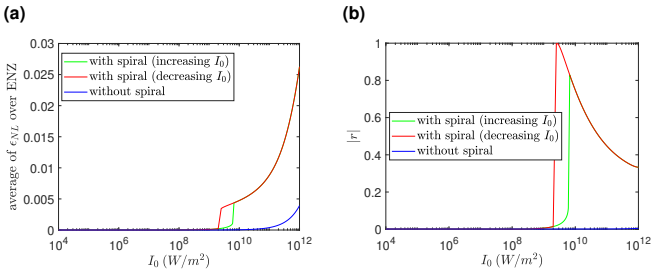

Fig. 4. Further enhanced nonlinearity obtained from doping an ENZ medium with a zero-area PEC inclusion. The geometry depicted in Fig. 3a is simulated, except for the nonlinearity introduced in the ENZ given by $\epsilon_{ENZ}(|\vec{E}|) = 10^{-6} + \frac{3\chi^{(3)}|\vec{E}|^2}{\epsilon_0}$ where $\chi^{(3)} = 10^{-29}\ (C.m/V^3)$[28]. (a) The nonlinear change in permittivity, averaged over the ENZ, in the presence and absence of the zero-area PEC spiral. (b) The reflection coefficient magnitude in the presence and absence of the zero-area PEC spiral.

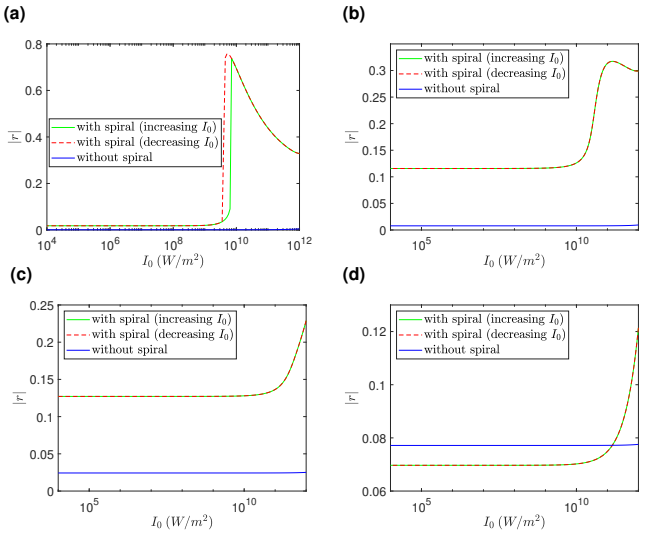

Fig. 5. The effect of ENZ loss on the enhanced nonlinearity studied in Fig. 4. The ENZ permittivity is given by $\epsilon_{ENZ}(|\vec{E}|) = 10^{-6} + i\epsilon''_{ENZ} + \frac{3\chi^{(3)}|\vec{E}|^2}{\epsilon_0}$ where $\chi^{(3)} = 10^{-29}\ (C.m/V^3)$. (a) $\epsilon''_{ENZ} = 10^{-3}$. (b) $\epsilon''_{ENZ} = 10^{-2}$. (c) $\epsilon''_{ENZ} = 0.03$. (d) $\epsilon''_{ENZ} = 0.1$.

leading to two distinctive applications, namely, designing soft surfaces and transforming the electric field distribution inside the ENZ, thereby further enhancing the nonlinearity of ENZ media. Due to a lack of need for a unit cell, as opposed to earlier proposals, our approach may facilitate the design of soft surfaces with arbitrary geometry flexibility, including geometrical features with a small radius of curvature, in the limit of a lossless ENZ host. Moreover, we have shown that a properly designed zero-area PEC inclusion may create enhanced electric fields inside the ENZ host, resulting in further boosting the nonlinear response. Finally, we numerically illustrated that our technique for enhancing the nonlinearity may be applicable even in the presence of losses corresponding to realistic materials.

Funding. US Air Force Office of Scientific Research (AFOSR) (FA9550-14-1-0389); Office of Naval Research (N00014-16-1-2029); Spanish Ministry of Science, Innovation and Universities (MCIU/AEI/FEDER/UE., RTI2018-093714-J-I00)

Disclosures. The authors declare no conflicts of interest.
See Supplement 1 for supporting content.

REFERENCES

1. I. Liberal and N. Engheta, Nat. Photonics **11**, 149 (2017).
2. M. Silveirinha and N. Engheta, Phys. Rev. B **75**, 075119 (2007).
3. I. Liberal, A. M. Mahmoud, Y. Li, B. Edwards, and N. Engheta, Science **355**, 1058 (2017).
4. Z. Zhou, Y. Li, H. Li, W. Sun, I. Liberal, and N. Engheta, Nat. Commun. **10**, 1 (2019).
5. J. Luo, B. Liu, Z. H. Hang, and Y. Lai, Laser & Photonics Rev. **12**, 1800001 (2018).
6. E. Nahvi, I. Liberal, and N. Engheta, ACS Photonics **6**, 2823 (2019).
7. E. Nahvi, I. Liberal, and N. Engheta, "Nonlinear tunability and mechanical actuation in photonically doped enz metasurfaces," in *2018 Conference on Lasers and Electro-Optics (CLEO)*, (IEEE, 2018), pp. 1–2.
8. J. Luo, J. Li, and Y. Lai, Phys. Rev. X **8**, 031035 (2018).
9. Z. Zhou, Y. Li, E. Nahvi, H. Li, Y. He, I. Liberal, and N. Engheta, Phys. Rev. Appl. **13**, 034005 (2020).
10. Y. Zhang, Y. Luo, J. Pendry, and B. Zhang, Phys. review letters **123**, 067701 (2019).
11. W. Ji, D. Wang, S. Li, Y. Shang, W. Xiong, L. Zhang, and J. Luo, Appl. Phys. A **125**, 129 (2019).
12. O. Reshef, I. De Leon, M. Z. Alam, and R. W. Boyd, Nat. Rev. Mater. **4**, 535 (2019).
13. T. S. Luk, D. De Ceglia, S. Liu, G. A. Keeler, R. P. Prasankumar, M. A. Vincenti, M. Scalora, M. B. Sinclair, and S. Campione, Appl. Phys. Lett. **106**, 151103 (2015).
14. A. Capretti, Y. Wang, N. Engheta, and L. Dal Negro, Opt. letters **40**, 1500 (2015).
15. M. Z. Alam, I. De Leon, and R. W. Boyd, Science **352**, 795 (2016).
16. L. Caspani, R. Kaipurath, M. Clerici, M. Ferrera, T. Roger, J. Kim, N. Kinsey, M. Pietrzyk, A. Di Falco, V. M. Shalaev, A. Boltasseva, and D. Faccio, Phys. review letters **116**, 233901 (2016).
17. A. Capretti, Y. Wang, N. Engheta, and L. Dal Negro, ACS Photonics **2**, 1584 (2015).
18. M. Clerici, N. Kinsey, C. DeVault, J. Kim, E. G. Carnemolla, L. Caspani, A. Shaltout, D. Faccio, V. Shalaev, A. Boltasseva, and M. Ferrera, Nat. communications **8**, 1 (2017).
19. E. G. Carnemolla, V. Bruno, L. Caspani, M. Clerici, S. Vezzoli, T. Roger, C. DeVault, J. Kim, A. Shaltout, V. Shalaev, A. Boltasseva, D. Faccio, and M. Ferrera, "Giant nonlinear frequency shift in epsilon-near-zero aluminum zinc oxide thin films," in *CLEO: Science and Innovations,* (Optical Society of America, 2018), pp. SM4D–7.
20. P.-S. Kildal, Electron. Lett. **24**, 168 (1988).
21. P.-S. Kildal, IEEE Transactions on Antennas Propag. **38**, 1537 (1990).
22. S. Maci and P.-S. Kildal, "Hard and soft gangbuster surfaces," in *Proc. URSI Int. Symp. Electromagnetic Theory,* (2004), pp. 290–292.
23. E. Rajo-Iglesias, Ó. Quevedo-Teruel, and L. Inclan-Sanchez, IEEE Transactions on Antennas Propag. **57**, 3852 (2009).
24. E. Rajo-Iglesias, L. Inclán-Sánchez, and O. Quevedo-Teruel, Prog. In Electromagn. Res. **6**, 123 (2009).
25. Z. Ying, P.-S. Kildal, and A. Kishk, "Bandwidth of some artificially soft surfaces," in *IEEE Antennas and Propagation Society International Symposium. 1995 Digest,* , vol. 1 (IEEE, 1995), pp. 390–393.
26. Z. Šipuš, H. Merkel, and P.-S. Kildal, IEE Proceedings-Microwaves, Antennas Propag. **144**, 321 (1997).
27. "COMSOL Multiphysics® v. 5.4. www.comsol.com. COMSOL AB, Stockholm, Sweden." .

28. B. E. Saleh and M. C. Teich, *Fundamentals of photonics* (John Wiley & Sons, 2019).
29. J. Kim, A. Dutta, G. V. Naik, A. J. Giles, F. J. Bezares, C. T. Ellis, J. G. Tischler, A. M. Mahmoud, H. Caglayan, O. J. Glembocki, A. V. Kildishev, J. D. Caldwell, A. Boltasseva, and N. Engheta, Optica. **3**, 339 (2016).

FULL REFERENCES

1. I. Liberal and N. Engheta, "Near-zero refractive index photonics," Nat. Photonics **11**, 149 (2017).
2. M. Silveirinha and N. Engheta, "Design of matched zero-index metamaterials using nonmagnetic inclusions in epsilon-near-zero media," Phys. Rev. B **75**, 075119 (2007).
3. I. Liberal, A. M. Mahmoud, Y. Li, B. Edwards, and N. Engheta, "Photonic doping of epsilon-near-zero media," Science **355**, 1058–1062 (2017).
4. Z. Zhou, Y. Li, H. Li, W. Sun, I. Liberal, and N. Engheta, "Substrate-integrated photonic doping for near-zero-index devices," Nat. Commun. **10**, 1–8 (2019).
5. J. Luo, B. Liu, Z. H. Hang, and Y. Lai, "Coherent perfect absorption via photonic doping of zero-index media," Laser & Photonics Rev. **12**, 1800001 (2018).
6. E. Nahvi, I. Liberal, and N. Engheta, "Nonperturbative effective magnetic nonlinearity in enz media doped with kerr dielectric inclusions," ACS Photonics **6**, 2823–2831 (2019).
7. E. Nahvi, I. Liberal, and N. Engheta, "Nonlinear tunability and mechanical actuation in photonically doped enz metasurfaces," in *2018 Conference on Lasers and Electro-Optics (CLEO),* (IEEE, 2018), pp. 1–2.
8. J. Luo, J. Li, and Y. Lai, "Electromagnetic impurity-immunity induced by parity-time symmetry," Phys. Rev. X **8**, 031035 (2018).
9. Z. Zhou, Y. Li, E. Nahvi, H. Li, Y. He, I. Liberal, and N. Engheta, "General impedance matching via doped epsilon-near-zero media," Phys. Rev. Appl. **13**, 034005 (2020).
10. Y. Zhang, Y. Luo, J. Pendry, and B. Zhang, "Transformation-invariant metamaterials," Phys. review letters **123**, 067701 (2019).
11. W. Ji, D. Wang, S. Li, Y. Shang, W. Xiong, L. Zhang, and J. Luo, "Photonic-doped epsilon-near-zero media for coherent perfect absorption," Appl. Phys. A **125**, 129 (2019).
12. O. Reshef, I. De Leon, M. Z. Alam, and R. W. Boyd, "Nonlinear optical effects in epsilon-near-zero media," Nat. Rev. Mater. **4**, 535–551 (2019).
13. T. S. Luk, D. De Ceglia, S. Liu, G. A. Keeler, R. P. Prasankumar, M. A. Vincenti, M. Scalora, M. B. Sinclair, and S. Campione, "Enhanced third harmonic generation from the epsilon-near-zero modes of ultrathin films," Appl. Phys. Lett. **106**, 151103 (2015).
14. A. Capretti, Y. Wang, N. Engheta, and L. Dal Negro, "Enhanced third-harmonic generation in si-compatible epsilon-near-zero indium tin oxide nanolayers," Opt. letters **40**, 1500–1503 (2015).
15. M. Z. Alam, I. De Leon, and R. W. Boyd, "Large optical nonlinearity of indium tin oxide in its epsilon-near-zero region," Science **352**, 795–797 (2016).
16. L. Caspani, R. Kaipurath, M. Clerici, M. Ferrera, T. Roger, J. Kim, N. Kinsey, M. Pietrzyk, A. Di Falco, V. M. Shalaev, A. Boltasseva, and D. Faccio, "Enhanced nonlinear refractive index in ε-near-zero materials," Phys. review letters **116**, 233901 (2016).
17. A. Capretti, Y. Wang, N. Engheta, and L. Dal Negro, "Comparative study of second-harmonic generation from epsilon-near-zero indium tin oxide and titanium nitride nanolayers excited in the near-infrared spectral range," ACS Photonics **2**, 1584–1591 (2015).
18. M. Clerici, N. Kinsey, C. DeVault, J. Kim, E. G. Carnemolla, L. Caspani, A. Shaltout, D. Faccio, V. Shalaev, A. Boltasseva, and M. Ferrera, "Controlling hybrid nonlinearities in transparent conducting oxides via two-colour excitation," Nat. communications **8**, 1–7 (2017).
19. E. G. Carnemolla, V. Bruno, L. Caspani, M. Clerici, S. Vezzoli, T. Roger, C. DeVault, J. Kim, A. Shaltout, V. Shalaev, A. Boltasseva, D. Faccio, and M. Ferrera, "Giant nonlinear frequency shift in epsilon-near-zero aluminum zinc oxide thin films," in *CLEO: Science and Innovations,* (Optical Society of America, 2018), pp. SM4D–7.
20. P.-S. Kildal, "Definition of artificially soft and hard surfaces for electromagnetic waves," Electron. Lett. **24**, 168–170 (1988).
21. P.-S. Kildal, "Artificially soft and hard surfaces in electromagnetics," IEEE Transactions on Antennas Propag. **38**, 1537–1544 (1990).
22. S. Maci and P.-S. Kildal, "Hard and soft gangbuster surfaces," in *Proc. URSI Int. Symp. Electromagnetic Theory,* (2004), pp. 290–292.
23. E. Rajo-Iglesias, Ó. Quevedo-Teruel, and L. Inclan-Sanchez, "Planar soft surfaces and their application to mutual coupling reduction," IEEE Transactions on Antennas Propag. **57**, 3852–3859 (2009).
24. E. Rajo-Iglesias, L. Inclán-Sánchez, and O. Quevedo-Teruel, "Back radiation reduction in patch antennas using planar soft surfaces," Prog. In Electromagn. Res. **6**, 123–130 (2009).
25. Z. Ying, P.-S. Kildal, and A. Kishk, "Bandwidth of some artificially soft surfaces," in *IEEE Antennas and Propagation Society International Symposium. 1995 Digest,* vol. 1 (IEEE, 1995), pp. 390–393.
26. Z. Šipuš, H. Merkel, and P.-S. Kildal, "Green's functions for planar soft and hard surfaces derived by asymptotic boundary conditions," IEE Proceedings-Microwaves, Antennas Propag. **144**, 321–328 (1997).
27. "COMSOL Multiphysics® v. 5.4. www.comsol.com. COMSOL AB, Stockholm, Sweden." .
28. B. E. Saleh and M. C. Teich, *Fundamentals of photonics* (John Wiley & Sons, 2019).
29. J. Kim, A. Dutta, G. V. Naik, A. J. Giles, F. J. Bezares, C. T. Ellis, J. G. Tischler, A. M. Mahmoud, H. Caglayan, O. J. Glembocki, A. V. Kildishev, J. D. Caldwell, A. Boltasseva, and N. Engheta, "Role of epsilon-near-zero substrates in the optical response of plasmonic antennas," Optica. **3**, 339–346 (2016).